Atomic structure of misfit dislocations at InAs/GaAs(110)

2008 J. Phys.: Condens. Matter 20 235227

(http://iopscience.iop.org/0953-8984/20/23/235227)

J. Phys.: Condens. Matter **20** (2008) 235227 (7pp) doi:10.1088/0953-8984/20/23/235227

Atomic structure of misfit dislocations at InAs/GaAs(110)

R Choudhury[1,4], **D R Bowler**[1,2,3] **and M J Gillan**[1,2,3]

[1] Department of Physics and Astronomy, University College London, Gower Street, London WC1E 6BT, UK
[2] Materials Simulation Laboratory, University College London, Gower Street, London WC1E 6BT, UK
[3] London Centre for Nanotechnology, University College London, 17-19 Gordon Street, London WC1H 0AH, UK

E-mail: rathin.choudhury@kcl.ac.uk, david.bowler@ucl.ac.uk and m.gillan@ucl.ac.uk

Received 1 April 2008, in final form 11 April 2008
Published 9 May 2008
Online at stacks.iop.org/JPhysCM/20/235227

Abstract
Heteroepitaxy of InAs on GaAs(110) leads to the formation of subsurface misfit dislocations to relieve strain. These dislocations have been observed both with transmission electron microscopy (TEM) and scanning tunnelling microscopy (STM), and show regular spacing. Electronic structure calculations of the structure of the core of the dislocations, as well as their location within the epitaxial layer, are presented. The most stable location is found to be at the interface, with the core centred over In. Calculated strain profiles and the thickness at which dislocations should form are in good agreement with available experimental data.

(Some figures in this article are in colour only in the electronic version)

1. Introduction

The technique of molecular beam epitaxy (MBE) is commonly used for the fabrication of thin film structures to within monolayer (ML) precision. The specific application of heteroepitaxy, in which substrate and growth material differ, has advanced many different technologies such as laser diodes, high-frequency transistors and fibre-optic communications, for example InGaAs/GaAs is itself a heterostructure commonly used in fibre-optic detectors. There is a strong interest in epitaxial growth of InAs on substrates such as GaAs(110), as such systems can act as patterned substrates for photonic applications [1].

Experiments reveal that 2d layer-by-layer growth occurs during the epitaxy of InAs on a GaAs(110) substrate [2–4]. Due to the large (7.2%) lattice constant mismatch between the two materials there is a build up of compressive strain energy in the deposited InAs (experimentally $L_{\mathrm{InAs}} = 6.06$ Å, $L_{\mathrm{GaAs}} = 5.65$ Å). There is very little intermixing of the In and Ga during growth, so that the epilayers are homogeneous InAs [4]. Eventually plastic deformation of the InAs occurs through the formation of strain relieving dislocations, as revealed by transmission electron microscopy (TEM) and scanning tunnelling microscopy (STM) [2–4]. In STM images, the dislocations appear as dark stripes or depressions on the surface, as illustrated in figure 1. These are seen after three InAs layers have been deposited, and have line vectors lying along [001], and Burgers vectors lying along $(a_0/2)[1\bar{1}0]$. The dislocations form a periodic array in the [001] direction with an average spacing of 60 Å. In addition, 60° dislocations are seen after coverage, θ, exceeds ∼20 ML, allowing relief of mismatch strain along the [001] direction also.

Additional STM studies and density functional theory (DFT) calculations of the core structures of the edge dislocations have been reported [5], predicting a core at the first epilayer including a five-coordinated In atom on the basis of *ab initio* calculations. A mean field theory for the strain relaxation kinetics has also been applied to reproduce the experimental dislocation strain profile [6], although this cannot predict the dislocation core structure in the atomistic sense. A phenomenological theory to predict θ_{crit}, the critical epilayer thickness at which dislocations should appear, has also been described [7], combining DFT calculations with a classical elasticity approach, obtaining θ_{crit} equal to 2.35 ML, conforming to experimental results, in which the dislocations are found to appear only after a minimum deposition of three InAs epilayers.

[4] Present address: Physics Department, King's College London, London, Strand WC2R 2LS, UK.

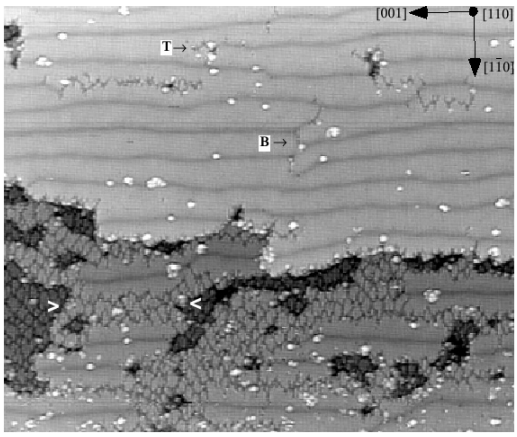

Figure 1. STM image of 5 ML of InAs on GaAs(110). The misfit dislocations are clearly visible as dark depressions, lying along [001]. Reprinted with permission from [4]. Copyright (1998) by the American Physical Society.

Experiments have been interpreted to suggest [3] that the edge dislocations form in the second layer or above due to their appearance at $\theta = 3$, but other authors [7] conclude that the dislocations are at the heterointerface itself. Our study directly calculates and compares the energies of dislocation networks in both layers to see which is energetically favoured, and then we compute θ_{crit}.

The structure of this paper is as follows: in section 2 we describe the DFT techniques and approximations used to perform calculations on the III–V systems. In section 3 we discuss our calculations on the semiconductor bulk and the (110) surfaces, before presenting the edge dislocation calculations in section 4. Finally in section 5 we present the conclusions of our study.

2. Methodology

Plane-wave pseudopotential DFT is capable of calculating accurate ground state energies for a wide variety of materials, and has successfully performed relaxations of many different types of defects and surfaces, as well as misfit dislocations [5, 8]. Its quantum accuracy is needed to successfully compute the relative energies of the different misfit dislocation structures which we examine, since effects such as charge transfer are insufficiently described by alternative approaches such as tight binding. In fact, our own attempts to model the dislocation reconstruction using tight binding failed, yielding unphysical structures, probably due to its limited ability to describe charge transfer.

We perform DFT calculations using the VASP plane-wave pseudopotential code [9], and its accompanying library of ultrasoft (US) pseudopotentials. An important issue concerning the pseudopotentials of In and Ga is whether to include the Ga 3d and the In 4d electrons in the valence set, rather than confining them to the pseudopotential. In [10] the effect of including the d electrons in the Ga valence set on the properties of GaN is examined, and is found to alter the lattice constants and cohesive energies (due to energy resonance of Ga 3d states with nitrogen 2s states [10]), thus we also examine the effect of including the d electrons. However, previous studies of the effect of including the d electrons in the Ga wavefunction for the calculation of the optical properties of GaAs have shown no important effect on results [11]. Our tests on the effects of the different pseudopotentials on the lattice constants and cohesive energies of the bulk crystals are given in section 3.1. The Ga(In) pseudopotentials not containing the 3d(4d) electrons are hereafter referred to as 3 electron pseudopotentials, in contrast with the alternative 13 electron pseudopotentials.

During geometry optimization forces were converged below a maximum of 0.02 eV Å^{-1}. The plane-wave threshold for all calculations was fixed at 13.26 Ryd, at which bulk lattice constants and energies (as well as energy differences) were found to be well converged. Using this cut-off we obtain bulk cohesive energies and surface energies in good agreement with the previous literature, as shown in section 3.1.

The energies calculated by the VASP code are by default relative to the energies of the isolated atoms in a non-spin-polarized ground state. In order to obtain energies to compare with experiment, one must calculate energies relative to spin-polarized ground states which are separately computed. When comparing our results against previous literature we quote energies relative to the correct spin-polarized atomic ground states; however, this distinction is not relevant for calculations of the relative energies of dislocations as it does not affect energy differences.

Calculations were performed on three types of system: the bulk semiconductors; the individual (110) surfaces; and finally on slabs containing misfit dislocations. Studies of the bulk and surface structures were necessary to develop the simulations on the more complex misfit dislocation networks. Bulk calculations were performed with cubic cells containing eight atoms and a **k**-point mesh of $8 \times 8 \times 8$ which converged the energies and lattice constants.

For surface calculations a vacuum gap of 5 Å was found to prevent unwanted interaction between slabs in the periodic supercell, the surface itself was modelled with a single repeat unit along the [1$\bar{1}$0] and [001] directions. Calculations were converged with an $8 \times 8 \times 1$ **k**-point mesh, a single **k**-point being sufficient along the slab normal. We found the geometry of a GaAs surface slab containing a minimum of seven layers to be well converged, by measuring characteristic surface parameters as a function of the slab thickness. These results are discussed in more depth in section 3.2.

Edge dislocation networks were represented by periodic supercells containing one misfit dislocation per 15 GaAs pairs along [1$\bar{1}$0], which is the perpendicular to the core (one dislocation per ≈60 Å), and only a single repeating unit along the dislocation line [001] direction. The number of GaAs substrate layers was fixed at 7, as chosen from calculations on the III–V surfaces. For cells ≈60 Å wide along [1$\bar{1}$0] a **k**-point mesh of $8 \times 1 \times 1$ converged total energies and geometries. Calculations on the misfit dislocations were performed using the generalized gradient approximation (GGA) only, due to limitations in computer time; GGA is expected to be more accurate for energy differences in

Table 1. Lattice constant and cohesive energy for bulk GaAs for different pseudopotentials and functionals (LDA and GGA).

GaAs	Lattice constant (Å)	Cohesive pair energy (eV)
LDA	5.59	−8.14
GGA	5.72	−6.51
GGA 3d	5.75	−6.43
EXPT	5.65	−6.52

Table 2. Lattice constant and cohesive energy for bulk InAs for different pseudopotentials and functionals (LDA and GGA).

InAs	Lattice constant (Å)	Cohesive pair energy (eV)
LDA	6.01	−7.55
GGA	6.17	−5.94
GGA 4d	6.18	−5.87
EXPT	6.06	−6.06

these systems (that is, the energies of reconstructions at the dislocation core). Calculations on the bulk and surface slabs were performed with both GGA and the local density approximation (LDA). In all simulations we use the theoretical III–V lattice constants rather than the experimental values to maintain consistency within our calculations. This leads to differences between the amount of strain in our simulations and in experiment, as well as a slightly different dislocation spacing, since we are exploring a consistent model system within GGA, to gain insight into the experimental findings.

3. Bulk and surface studies

3.1. Bulk crystals

We calculate the properties of the bulk III–Vs, such as lattice constants and cohesive energies, for comparison with experiment. We also examine the effects of strain on the properties of bulk InAs, since the InAs which is initially deposited onto the GaAs(110) substrate is compressed in the (110) plane. After the edge misfit dislocations have formed, the InAs epilayers remain compressed along [001] only. Thus we calculate the cohesive energy and (110) interlayer spacings of bulk InAs under both uniaxial [001] and biaxial strain.

In table 1 we summarize our results on the GaAs bulk. GGA calculations are performed with both 13 electron and 3 electron pseudopotentials, and both GGA pseudopotentials give similar results, thus for calculations on misfit dislocations we use the three electron GGA pseudopotential for expediency. The cohesive energy obtained using GGA is closer to the experimental value than LDA, which overestimates it. Note that the energies presented are per III–V pair, and are relative to the ground state energies of the isolated atoms. The error in the lattice constant is similar for both LDA and GGA, with GGA overestimating and LDA underestimating the experimental value. Values of the cohesive energy are in good agreement with previous *ab initio* results [12, 13].

Table 2 shows the lattice constants and cohesive energies of equilibrium bulk InAs. As for GaAs both types of GGA pseudopotential provide similar results, and we again choose to use the 3e GGA pseudopotential for the misfit dislocation calculations. The LDA and GGA results for the cohesive energy and lattice constant match the trend seen for GaAs, the GGA value of the cohesive energy being closer to the experimental value than the LDA. The error in the GGA lattice constant is larger than that of LDA, and again overestimates the experimental value. The lattice constant mismatch between the two semiconductors gives rise to a compressive strain experimentally valued at 7.2%. The corresponding LDA value is 7.5%, and the GGA value is 7.9%, reflecting the different equilibrium lattice constants of the two approximations. This difference in the strain will affect the value of θ_{crit} in section 4, as we work with the theoretical GGA lattice constants, but we anticipate that the essential physics at the dislocation core will not be changed by the GGA strain being higher than the experimental value.

Table 3. Interlayer spacing and cohesive energy for bulk InAs under different strain conditions.

III–V crystal	(110) spacing (Å)	Energy per pair (eV)
GaAs	2.02	−8.0
InAs	2.18	−7.82
Uniaxially strained InAs	2.27	−7.77
Biaxially strained InAs	2.32	−7.63

Table 3 summarizes the (110) interlayer spacings and cohesive energies for InAs under uniaxial and biaxial strain states, including the results for equilibrium InAs and GaAs for comparison. For biaxial strain the InAs was constrained to the theoretical GaAs lattice parameter of 5.7216 Å along both [001] and $[1\bar{1}0]$, its own theoretical lattice parameter being 6.1664 Å. The (110) spacing of the biaxially strained bulk increases to 2.32 Å, 0.14 Å greater than the equilibrium value. The cohesive energy per InAs pair, −7.63 eV, is 0.19 eV higher (less stable) than for unstrained InAs.

The strained InAs is placed initially at the GaAs lattice sites during our simulations, and the atoms undergo a small displacement away from these under the compressive strain. Thus the bond length in the (110) plane is no longer equal to that of bulk GaAs (2.48 Å), but increases to 2.58 Å. For the case of uniaxial strain, the InAs is constrained to the GaAs lattice constant along [001] only. In table 3 we see that the minimum energy, −7.77 eV, lies between that of the equilibrium (−7.82 eV) and biaxially strained value (−7.63 eV). The edge dislocations relieve strain along $[1\bar{1}0]$ but considerable residual strain energy will remain in the epilayers after formation of the edge dislocations. Though this strain is relieved by a network of 60° dislocations, they form after many tens of epilayers have been deposited, and we do not consider this aspect of the strained growth. The equilibrium interplanar spacing, 2.27 Å, is also between that of the relaxed bulk (2.18 Å) and biaxially strained values (2.32 Å). This is expected, since the vertical expansion correlates with the total amount of strain.

3.2. (110) surface calculations

The accuracy of our surface relaxations is important as we will be calculating the surface strain field of the dislocations,

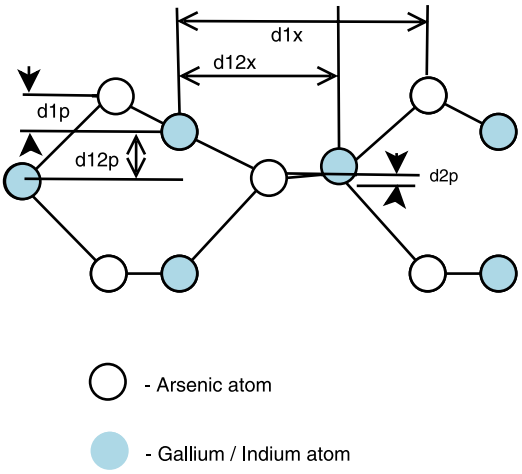

Figure 2. Characteristic displacements of atoms in the III–V (110) surface.

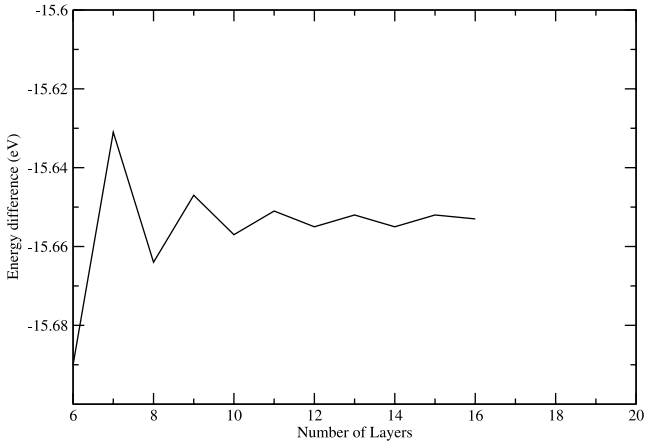

Figure 3. Convergence of slab energy differences for InAs (eV).

Table 4. Characteristic geometric parameters of the GaAs (110) surface as illustrated in figure 2.

Author	d1p	d1x	d2p	d12p	d12x
Ours	0.69	4.470	0.104	1.463	3.259
Qian *et al*	0.58	4.390	0.07	1.440	3.180
Alves *et al*	0.67	4.407	0.098	1.415	3.180
Meyer *et al* [14] (expt)	0.69	4.518	0.120	1.442	3.339

and we must obtain the minimum number of layers needed to make the GaAs substrate a reliably approximate semi-infinite bulk. The (110) surface contains equal numbers of group III and group V atoms, and is thus charge neutral or non-polar, having the periodicity of the underlying bulk. Experimental observations [14, 15] reveal that in III–V semiconductors the group V atoms are pushed upwards out of the surface plane whilst the group III atoms are drawn inwards, creating a characteristic tilting of the unit cell, as in figure 2. The Ga(In) and As surface atoms are three-fold coordinated and the Ga relaxes into an sp^2 hybridization while As moves into an sp^3 hybridization and has a lone pair. The strain effects of this tilt do not penetrate more than a few layers into the underlying bulk, which we confirm by measuring the decreasing tilting of successive layers into the bulk. The geometries of the (110) surfaces of InAs and GaAs have previously been treated using DFT [16, 14, 17], to reproduce experimental results [18]. The geometric parameters conventionally used to describe the surface are shown in figure 2, and we give our results in terms of these.

We measure the parameters as a function of the number of layers in our surface slab, finding that a total of seven layers, all free to relax, is sufficient for approximating the substrate bulk. For each additional layer after the seventh the maximum fractional change in the parameters is roughly 1%. We present a comparison of our obtained GaAs (LDA) geometry against previous authors' work [14, 16, 17] in table 4. Our results are in good agreement with experiment and previous calculations.

We also calculated the cleavage energy of the (110) surfaces of GaAs and InAs within both the LDA and GGA approximations. The energy of a slab with two surfaces can be written:

$$E_{\text{slab}} = E_{\text{bulk}} + 2E_{\text{surface}}. \quad (1)$$

The slab is effectively a piece of bulk crystal with an additional (positive) energy due to the relaxation of its two surfaces. In order to isolate E_{surface} we can obtain E_{bulk} in a separate calculation and subtract it from E_{slab} [16].

Within an LDA calculation we obtain a surface energy of 50 meV Å^{-2} for GaAs(110), in good agreement with previous LDA results [19, 16]. The experimental value is 54 ± 9 meV Å^{-2} [18]. Using GGA we find a lower value of 38 meV Å^{-2}. In fact we find a similar trend for the InAs (110) surface energy using LDA and GGA functionals, finding a value of 32.1 meV Å^{-2} with GGA and 41.2 meV Å^{-2} with LDA. In both cases the surface energy is lower than that of GaAs. Our LDA value is in good agreement with that of Moll *et al* [19] who obtained 41 meV Å^{-2}. It appears that GGA underestimates the surface energy relative to LDA, and is further from the experimental value; there is a growing body of evidence [20–22] that this is a general feature of GGA.

We can also see whether the centre of the surface slab is bulk-like by examining the energetic cost of adding extra layers. Once the slab centre is bulk-like the energy cost of an additional layer will be exactly equivalent to the cost of adding a layer to the periodic bulk. A plot of the slab energy differences (the total energy difference between a slab with n layers and a slab with $n - 1$ layers) for InAs is shown in figure 3. There are four atoms in each layer and the energy differences converge towards the bulk value of -7.82 eV (note the factor of two difference due to the tabulated value being per InAs pair), presented in table 3. Figure 3 shows us that the geometry and energy are not perfectly converged by seven layers, but due to computational limits seven substrate layers are used in our simulations of the heteroepitaxy. This is not expected to have a significant effect on our conclusions, however, as the geometric parameters are converged to within 1%, and differences of meV will not affect our final results.

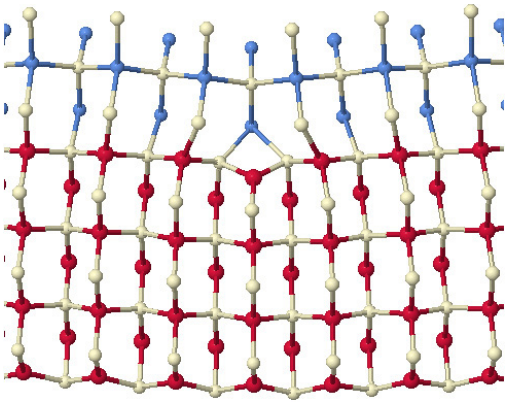

Figure 4. Structure of dislocation core at the first layer. The As atoms are represented by cream (light grey) spheres, Ga atoms by red (dark grey) spheres and In atoms by blue (medium grey) spheres.

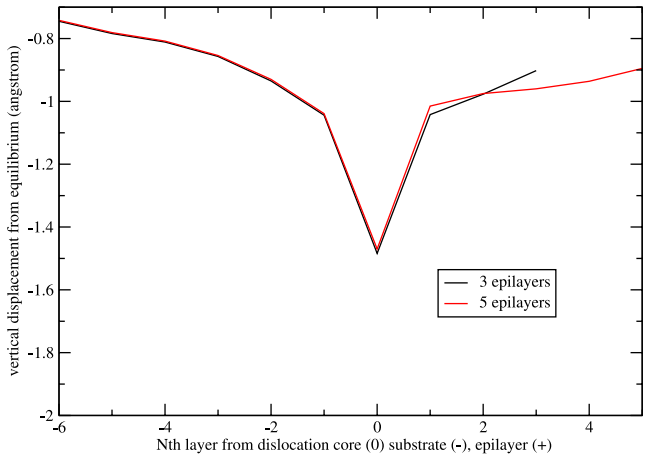

Figure 5. Magnitude of the vertical displacement of atoms centred along the dislocation line. Results for the cell with three layers of InAs are indicated with a black line, results with five layers with a grey line.

3.3. Strained InAs surface energy

We also calculate the surface energy of biaxially strained InAs, as discussed in section 3.1. One must be careful to include enough vacuum to take into account the vertical expansion of the InAs during the simulation. After relaxations it was confirmed that there were at least 5 Å of vacuum between neighbouring surfaces, which was sufficient to isolate the slabs. The energy differences between strained InAs slabs of increasing thickness converge towards the cohesive energy of the biaxially strained bulk, −7.63 eV. The value of the surface energy is 25 meV Å^{-2}. This is lower than the unstrained InAs (110) surface energy of 32 meV Å^{-2}. Previous studies of the (110) surface energy of strained InAs [19], have combined DFT calculations with classical elasticity theory to suggest that compressive strain lowers the (110) surface energy, in agreement with our calculation.

4. Misfit dislocations

Here we explain our construction of the misfit dislocations, and report the results of our calculations to obtain the lowest energy core from initial candidate structures. We then calculate the critical epilayer thickness at which dislocations are predicted to occur. The equilibrium spacing of the misfit dislocations determines the minimum width of our simulation cells and we find it in section 4.1.

4.1. Equilibrium spacing

Experimentally the dislocations were seen to be separated by an average of 60 Å [3]. The spacing of misfit dislocations can be calculated using the equation

$$S = \frac{100 b_{\text{edge}}}{m} \tag{2}$$

where m is the percentage misfit strain, and b the edge component of the Burgers vector, $a_0/\sqrt{2}$ in our case. Substituting in the experimental InAs Burgers vector the value of 7.2% for the misfit strain gives a spacing of ≈60 Å, which corresponds well to experiment.

We are working with the GGA lattice constants, so that the strain in our calculations is $\epsilon_{\text{th}} = 0.0786$, and the InAs Burgers vector is 4.36 Å, leading to a GGA equilibrium spacing of $d_{\text{gga}} = 55.5$ Å, slightly less than the experimental value. Thus we remove one row of InAs for every fifteen rows of GaAs to form the misfit dislocations in our simulations. The GGA and experimental spacings are quite similar, and we anticipate that the difference in the theoretical and experimental strain values will not significantly affect the validity of our results.

4.2. Preferred epilayer

In [3] it is suggested that the core should sit in the second layer or above, since no threading component links the dislocations to the surface, so that they must lie directly below the InAs layer thickness (3 ML) at which they first appear. However it is also suggested that they lie within the first epilayer [23]. Thus we calculate the lowest energy position for the dislocation core in order to clarify this uncertainty. This may be framed within two separate questions: first, which is the energetically preferred layer; second, is a core centred on In or As lowest in energy?

Figure 4 shows the relaxed structure of an In centred core in the first epilayer, with the In atom shaded in blue. Essentially it is identical to that obtained in [23], also using DFT. The reconstruction results in the indium atom forming bonds to five arsenic atoms, rather than four. The gallium immediately beneath the core moves down into the substrate, retaining bonds to only three arsenic atoms.

The dislocation causes a vertical depression of atoms from their original positions. We measure this in a given layer by subtracting an atom's z coordinate from that of the highest atom of the same species in the same layer. The species must be the same to account for the tilting of the (110) surface. The highest (least displaced) atoms are halfway between dislocation cores, and are also the least strained along $[1\bar{1}0]$ relative to their neighbours in the layer below. In figure 5 we have plotted the vertical dip of atoms along the dislocation

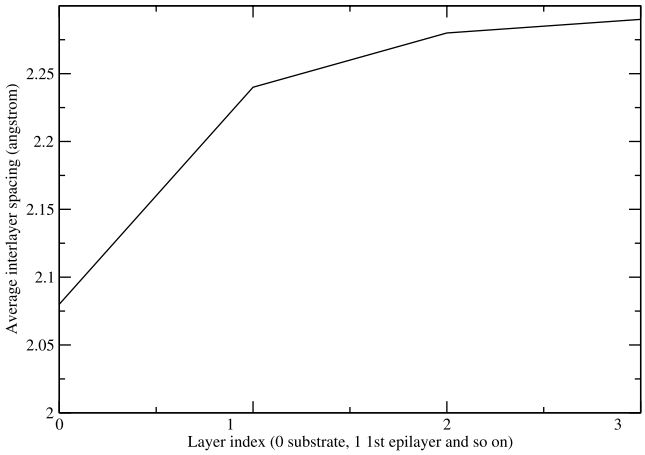

Figure 6. InAs interlayer spacing from one to three epilayers, for a dislocation core at the interface.

core line as a function of layer. The maximum displacements are for atoms immediately at the dislocation core. The 0.9 Å magnitude of the surface dip remains unchanged whether there are three or five epilayers. This is slightly greater than the experimental value [4] of 0.7 Å, but our measurements do agree with the experimental result that the dip magnitude remains constant from three to five epilayers. Also STM measurements include electronic as well as height information, which could lead to a small discrepancy.

At the bottom layer of our GaAs substrate there is also a dip of 0.75 Å since the strain has not relaxed by the final substrate layer. One might argue that fixing the atoms of the bottom substrate layer in bulk positions during the relaxation would be a better way of performing the calculation, but this could induce artificial strains that affect results more than our seven layer slab approximation. Many more substrate layers would be required to capture the dislocation strain field (usually assumed to be of the order of the dislocation spacing, in this case 60 Å) and these were computationally unavailable.

We can characterize the compressive strain remaining in the InAs epilayers above the dislocation by measuring their (110) interlayer spacing. We plot the interlayer spacing as a function of epilayer in figure 6. It is averaged over the supercell width (the spacing is non-uniform across the supercell due to the strain field of the dislocation). The (110) spacing between the GaAs at the heterointerface and the layer beneath it is just 2.1 Å and it increases to a value of 2.28 Å between the third and fourth InAs epilayers. The value of 2.28 Å is very close to the equilibrium spacing for InAs under uniaxial strain, shown in table 3, which is 2.27 Å. This indicates that the InAs in epilayers above the misfit dislocation does indeed behave as if it were a uniaxially strained bulk. Note that the spacing between the fourth and fifth epilayers is not shown on the graph as it is strongly affected by the surface relaxation. Establishing that the InAs epilayers above the dislocation bear the characteristics of the bulk under uniaxial strain has important consequences for our later calculations comparing the energies of misfit dislocations with different core positions. When performing energy comparisons between

Table 5. Energies for dislocation cores at different positions; compensation energy for different numbers of InAs pairs is −7.77 eV.

Epilayer	First layer E	First layer $E + \mu$	Second layer E	$\Delta(1-2)$
3	−1182.60	−1190.37	−1189.66	0.71
4	−1291.70	−1299.47	−1298.43	1.04
5	−1400.42	−1408.19	−1407.04	1.15

different dislocation structures we can compensate for the different numbers of InAs pairs present in each system with the energy of a pair in the uniaxially strained bulk (7.77 eV).

We also compute the relaxed structure of a dislocation core at the second epilayer to see whether it is lower in energy than a core at the interface. Again, the In atom at the core is five-fold coordinated, and the In atom at the heterointerface below it attains three-fold coordination. The InAs layer at the surface dips by 0.9 Å due to the dislocation strain field, the same amount as for the first layer core.

There is one more InAs pair in the system containing a dislocation at the second layer, as it contains 15 InAs pairs at the interface rather than 14. Thus we cannot compare the total energies of the two systems directly, but must compensate for the energy of this 'missing pair', adding the pair energy of the uniaxially strained bulk, −7.77 eV, to the total energy of the dislocation at the first layer. The resulting values are shown in table 5. The first layer dislocation is consistently lower in energy, with a margin of 0.7 eV at $\theta = 3$ increasing to 1.5 eV by $\theta = 5$, thus it is the stablest configuration, agreeing with the assertion of [23]. The difference between the uniaxially and biaxially strained InAs energies is smaller than the difference between cores at different layers, so the result will be insensitive to any errors in these energies. This result does not rule out the possibility of kinetic effects producing a second layer core, but indicates a strong energetic drive to keep the dislocation at the interface.

4.3. Preferred atomic centre

The first layer dislocation may be centred on either In or As and thus we perform a geometry optimization of a core based on As to compare the total energy with the In centred core. During the relaxation, significant rebonding led to repositioning of the core over the neighbouring In rather than As, indicating that the core sits preferentially over In. The symmetry of the initial structure may have been broken due to very slight inaccuracies in the initial positions, but these were very small (less than thousandths of an Å), hardly enough to prejudice our calculations. In a repeat of the simulation we found the same result, confirming our conclusions that the core on As is unstable.

4.4. Critical epilayer thickness

We have demonstrated that the energetically preferred structure for the dislocation core is at the first epilayer, centred over In. We can obtain the critical thickness, θ_{crit} at which the dislocations should appear by comparing the total energy

Table 6. Energies for dislocation cores in the first epitaxial layer, compared to a perfect system (energies given in eV, per cell and per core).

n epilayers	$\Delta E_{\text{1st layer}}$	Correction	$\Delta E_{\text{1st layer}}$corrected
2	16.57	−15.54	1.03
3	22.56	−23.31	−0.75
4	28.24	−31.08	−2.84
5	33.59	−38.85	−5.26

Table 7. Energies for dislocation cores in second epitaxial layer, compared to a perfect system (energies given in eV, per cell and per core).

n epilayers	$\Delta E_{\text{2nd layer}}$	Correction	$\Delta E_{\text{2nd layer}}$ corrected
1	—	—	—
2	—	—	—
3	15.49	−15.54	−0.05
4	21.51	−23.31	−1.80
5	26.98	−31.08	−4.10

of dislocation systems against those containing coherently strained epilayers. The number of InAs pairs in the cells will differ due to the removal of InAs to form the dislocations, but we compensate by adding the value of −7.77 eV. In tables 6 and 7 we present the energies per dislocation (per simulation cell and per core).

The first layer dislocation lies lower in energy than the coherent epilayers once a total of three epilayers have been deposited, by −0.75 eV per cell. It is higher in energy by 1.03 eV when $\theta = 2$, and this reflects the energetic cost of the core reconstruction. A linear interpolation between these two values gives a value of $\theta_{\text{crit}} = 2.6$ for the critical number of epilayers. This differs slightly from the conclusions of [7] ($\theta_{\text{crit}} = 2.35$) but is in qualitative agreement, predicting the appearance of misfit dislocations once the third epilayer starts growing. However, our calculation takes a direct numerical approach, rather than fitting the DFT energies to find the parameters in classical energy-balance equations [7].

A similar analysis for dislocations lying in the second layer reveals only a very small difference in energy between the two systems once three epilayers have been deposited (−0.05 eV). Such a small value is not definitive as to whether such plastic deformation should occur on deposition of the third epilayer. However, by $\theta = 4$ we see that the second layer dislocation network becomes favourable with an energy difference of −1.80 eV. The small energy difference at $\theta = 3$ does not lend strong support to the assertion of [3] that the dislocations lie at the second epilayer and form a network once $\theta = 3$.

5. Discussion and conclusion

We have established the energetically preferred structure of misfit edge dislocations at the InAs/GaAs(110) heterointerface using DFT, finding a core centred on In in the first InAs epilayer to be lowest in energy. The In atom at the core is five-coordinated, and the Ga atom below is three-coordinated, in agreement with previous *ab initio* results [23]. A core centred on an As atom is unstable, spontaneously relaxing into one centred on In. Using DFT only, we directly compute the critical thickness at which the misfit dislocation network should first appear, finding $\theta_{\text{crit}} = 2.6$ ML. This is close to a previously calculated value of 2.35 ML [7], found through a combination of *ab initio* calculation and classical elasticity theory. Our value of θ_{crit} also agrees well with the experimental finding that the dislocation network appears after $\theta = 3$ ML [3]. We measure the magnitude of the surface depression due to the dislocation to be 0.9 Å which is close to the experimental value of 0.7 Å [4]. We observe no change in the magnitude of the depression on going from $\theta = 3$ to 5 which is also in agreement with the experimental observations [3]. Our results demonstrate the capability of DFT in directly calculating the energies of defects at strained thin film heterointerfaces of III–V semiconductors, with its close correspondence to experiment.

Acknowledgments

DRB is supported by the Royal Society. RC was supported by the EPSRC.

References

[1] Norman C E, Pratt A R, Williams R L, Fahy M R, Marinopoulou A and Chatenoud F 1995 *Inst. Phys. Conf. Ser.* **146** 737
[2] Zhang X, Pashley D W, Hart L, Neave J H, Fawcett P N and Joyce B A 1993 *J. Cryst. Growth.* **131** 300
[3] Belk J G, Sudijono J L, Zhang X M, Neave J H, Jones T S and Joyce B A 1997 *Phys. Rev. Lett.* **78** 475
[4] Belk J G, Pashley D W, Joyce B A and Jones T S 1998 *Phys. Rev.* B **58** 16194
[5] Oyama N, Ohta E, Kyozaburo T, Shiraishi K and Yamaguchi H 1999 *J. Cryst. Growth.* **201/202** 256
[6] Zepeda-Ruiz L, Maroudas D and Weinberg W 1999 *J. Appl. Phys.* **85** 3677
[7] Okajima K, Takeda K, Oyama N, Ohta E, Shiraishi K and Ohno T O 2000 *Japan. J. Appl. Phys.* **39** L917
[8] Cicero G, Pizzagalli L and Catellani A 2002 *J. Phys.: Condens. Matter* **14** 13031
[9] Kresse G and Furthmüller J 1996 *Phys. Rev.* B **54** 11169
[10] Fiorentini V, Methfessel M and Scheffler M 1993 *Phys. Rev.* B **47** 13353
[11] Monachesi P, Marini A, Onida G, Palummo M and Del Sole R 2001 *Phys. Status Solidi* a **184** 101
[12] Fuchs M, Bockstedte M, Pehlke E and Scheffler M 1998 *Phys. Rev.* B **57** 2134
[13] Juan Y M, Kaxiras E and Gordon R G 1995 *Phys. Rev.* B **51** 9521
[14] Meyer R J, Duke C B, Paton A, Kahn A, So E, Yeh J L and Mark P 1979 *Phys. Rev.* B **19** 5194
[15] Mailhiot C and Duke C B 1984 *Surf. Sci.* **149** 366
[16] Qian G X, Martin R M and Chadi D J 1988 *Phys. Rev.* B **37** 1303
[17] Alves J L A, Hebenstreit J and Scheffler M 1991 *Phys. Rev.* B **44** 6188
[18] Messmer C and Bilello J 1981 *J. Appl. Phys.* **52** 4623
[19] Moll N, Kley A, Pehlke E and Scheffler M 1996 *Phys. Rev.* B **54** 8844
[20] Mattson A E and Jennison D R 2002 *Surf. Sci. Lett.* **520** L611
[21] Yu D and Scheffler M 2004 *Phys. Rev.* B **70** 155417
[22] Alfé D and Gillan M 2006 *J. Phys.: Condens. Matter* **18** L435
[23] Oyama N, Ohta E, Takeda K, Shiraishi K and Yamaguchi H 1999 *Surf. Sci.* **433–435** 900